

1 Carbon flux and forest dynamics: increased deadwood
2 decomposition in tropical rainforest tree-fall gaps
3

4 **Running title:** Faster deadwood decay in canopy gaps
5

6 **Authors:** H. M. Griffiths¹, P. Eggleton², N. Hemming-Schroeder³, T.
7 Swinfield^{4,5}, J. S. Woon^{1, 2}, S. D. Allison^{3,6}, D.A. Coomes⁴, L. A. Ashton⁷ & C.
8 L. Parr^{1,8,9}

10 **Affiliations**

11 ¹ School of Environmental Sciences, University of Liverpool, Liverpool, L69 3GP, UK

12 ² Department of Life Sciences, Natural History Museum, London, UK

13 ³ Department of Earth System Science, University of California, Irvine, CA 92697, USA

14 ⁴ Department of Plant Sciences, University of Cambridge Conservation Research Institute,
15 Pembroke Street, Cambridge, CB2 3QZ, UK

16 ⁵ Centre for Conservation Science, Royal Society for the Protection of Birds, David
17 Attenborough Building, Pembroke Street, Cambridge, CB2, 3QZ, UK

18 ⁶ Department of Ecology and Evolutionary Biology, University of California, Irvine, CA
19 92697, USA

20 ⁷ School of Biological Sciences, The University of Hong Kong, Hong Kong SAR, China

21 ⁸ Department of Zoology & Entomology, University of Pretoria, Pretoria, South Africa

22 ⁹ School of Animal, Plant and Environmental Sciences, University of the Witwatersrand,
23 Wits, South Africa

24

25 Hannah Griffiths ORCID: 0000-0002-4800-8031

26 **Contact information**

27 Email: Hannah.griffiths@liverpool.ac.uk; Tel: +44 151 794 2000

28 **Abstract**

29 Tree mortality rates are increasing within tropical rainforests as a result of
30 global environmental change. When trees die, gaps are created in forest
31 canopies and carbon is transferred from the living to deadwood pools.
32 However, little is known about the effect of tree-fall canopy gaps on the
33 activity of decomposer communities and the rate of deadwood decay in
34 forests. This means that the accuracy of regional and global carbon
35 budgets is uncertain, especially given ongoing changes to the structure of
36 rainforest ecosystems. Therefore, to determine the effect of canopy
37 openings on wood decay rates and regional carbon flux, we carried out
38 the first assessment of deadwood mass loss within canopy gaps in old-
39 growth rainforest. We used replicated canopy gaps paired with closed
40 canopy sites in combination with macroinvertebrate accessible and
41 inaccessible woodblocks to experimentally partition the relative
42 contribution of microbes versus termites to decomposition within
43 contrasting understory conditions. We show that over a 12-month period,
44 wood mass loss increased by 63% in canopy gaps compared with closed
45 canopy sites and that this increase was driven by termites. Using LiDAR
46 data to quantify the proportion of canopy openings in the study region, we
47 modelled the effect of observed changes in decomposition within gaps on
48 regional carbon flux. Overall, we estimate that this accelerated
49 decomposition increases regional wood decay rate by up to 18.2%,
50 corresponding to a flux increase of $0.27 \text{ Mg C ha}^{-1} \text{ yr}^{-1}$ that is not currently
51 accounted for in regional carbon budgets. These results provide the first
52 insights into how small-scale disturbances in rainforests can generate

53 hotspots for decomposer activity and carbon fluxes. In doing so, we show
54 that including canopy gap dynamics and their impacts on wood
55 decomposition in forest ecosystems could help improve the predictive
56 accuracy of the carbon cycle in land surface models.

57

58 **Key words**

59 Termites; Invertebrates; Carbon cycling; Carbon modelling; Canopy gap;
60 Tree mortality; Disturbance; Global change

61

62 **Introduction**

63

64 Uncertainty in the behaviour of the carbon cycle is one of the biggest
65 limiting factors in accurately predicting Earth's temperature into the 21st
66 century (Bodman, Rayner, & Karoly, 2013). Tropical forests hold over half
67 of global forest carbon stocks (471 ± 93 PgC), 56% of which is stored in
68 biomass, and sequester 1.2 ± 0.4 PgC annually (Pan et al., 2011). Recent
69 work has highlighted how human pressures affect rainforest carbon stocks
70 in living and dead biomass, showing that selective logging and
71 degradation increase the proportion of deadwood stocks relative to living
72 biomass in African and Asian rainforests (Carlson, Koerner, Medjibe,
73 White, & Poulsen, 2017; Pfeifer et al., 2015).

74

75 Decomposition is the process by which the carbon in dead plant material
76 is assimilated into soil carbon stores, lost through leaching or released as
77 CO₂ into the atmosphere through respiration (Cornwell et al., 2009; Swift,
78 1977). Yet, despite the fact that decomposition has far reaching
79 implications for global carbon budgets (Hubau et al., 2020), it remains
80 poorly understood compared with other key ecosystem processes such as
81 primary production (Harmon, Bond-Lamberty, Tang, & Vargas, 2011).
82 Furthermore, what is known about the factors controlling deadwood decay
83 is geographically biased towards temperate regions, with tropical forest
84 decomposition studies representing just 14% of the published literature
85 (Harmon et al., 2020). This bias means we lack a basic understanding of

86 the factors that mediate the rate and fate of carbon turnover through
87 globally important deadwood stocks in tropical rainforests.

88

89 The effect of canopy openness represents an important source of
90 uncertainty in our understanding of the factors that affect the
91 decomposition of deadwood in forests (Harmon et al., 2020). This is a
92 major gap in understanding given that tree mortality rates are rising in
93 humid tropical forests (McDowell et al., 2018) as a result of increases in
94 the frequency and severity of hurricanes and drought (Cai et al., 2014);
95 continued selective logging and degradation (Baccini et al., 2017); and
96 increases in biotic agents of tree death (liana load, insect outbreaks and
97 disease; Allen, Breshears & McDowell 2015). Consequently, it is likely that
98 the size and frequency of rainforest canopy gaps are increasing, along
99 with concurrent changes in the volume and spatial distribution of
100 deadwood stocks (Carlson et al., 2017; Pfeifer et al., 2015). However,
101 because our knowledge of the effect of canopy gaps on deadwood decay
102 rates is currently limited to just two studies in temperate and boreal
103 forests (Janisch, Harmon, Chen, Fath, & Sexton, 2005; Shorohova &
104 Kapitsa, 2014), we lack an empirical evidence base from which to predict
105 the consequences of ongoing changes to the structure of tropical
106 rainforests for decomposition and carbon flux. Data shortages such as
107 these limit the capacity to resolve carbon budget imbalances because
108 information on how land-surface heterogeneity can affect carbon-cycling
109 and land-atmosphere interactions is a key area of uncertainty in Earth
110 system models (Lawrence *et al.* 2019). Therefore, there is a clear need to

111 improve our mechanistic understanding of the drivers of change in
112 rainforest carbon budgets and thus increase the accuracy and predictive
113 power of the land surface models included in Earth system models.

114

115 There is mounting evidence that termites along with microbes are the
116 major agents of deadwood decomposition in rainforest ecosystems (da
117 Costa, Hu, Li, & Poulsen, 2019; Griffiths, Ashton, Evans, Parr, & Eggleton,
118 2019; Liu et al., 2015). It is possible that treefall canopy gaps could
119 negatively or positively affect the activity of both groups. Habitat
120 disturbance and degradation reduces termite abundance and diversity
121 (Dibog, Eggleton, Norgrove, Bignell, & Hauser, 1999; Eggleton et al.,
122 1995; Ewers et al., 2015; Luke, Fayle, Eggleton, Turner, & Davies, 2014;
123 Tuma et al., 2019) while microbial-mediated nutrient mineralisation rates
124 decline in response to drought (Yavitt, Wright, & Wieder, 2004). Changes
125 to the structure of forests caused by removal of trees during selective
126 logging has been reported to increase microclimate heterogeneity and
127 create hotter and drier conditions in the forest understory (Blonder et al.,
128 2018; Hardwick et al., 2015). Therefore, the changes in understory
129 conditions caused by openings in the canopy when a tree dies could have
130 major negative effects on both termite and microbial mediated
131 decomposition. If this is the case, we expect decay rates to slow in canopy
132 gaps as result of disturbance and unfavourable microclimatic conditions
133 for the decomposer community. However, an alternative possibility is that
134 the high concentration of foraging resource (i.e. dead plant matter) in
135 canopy gaps, that result from tree death, may positively affect

136 decomposition processes by attracting termites and/or stimulating a
137 positive priming effect within the microbial community (e.g. Lyu et al.,
138 2018). Under this scenario, we expect to see an increase in decay rates in
139 canopy gaps in response to elevated resource availability where a tree
140 has fallen.

141

142 The overarching aim of this investigation was to determine if deadwood
143 decay rates differ in canopy gaps compared with closed canopy sites in
144 tropical rainforest. Additionally, we partitioned the relative contribution of
145 microbes and termites in driving deadwood mass loss in canopy openings
146 and estimated the effect of any changes in decomposition rates within
147 canopy gaps on regional carbon flux. To achieve this aim, we used
148 macroinvertebrate-accessible and inaccessible woodblocks placed within
149 tree fall canopy gaps and closed canopy sites in an old growth rainforest
150 in Malaysian Borneo. Furthermore, we assessed the termite community
151 composition and soil microclimatic conditions within experimental sites
152 and estimated the volume of deadwood associated with canopy gaps
153 compared with closed canopy sites. This unique experimental design
154 allowed us to test alternative hypotheses that deadwood
155 decomposition in canopy gaps could either: 1) decelerate due to a
156 negative effect of disturbance and a hotter, drier microclimate (e.g.
157 Blonder *et al.* 2018) leading to a reduction in the activity of the
158 decomposer community, or 2) accelerate in response to an influx of dead
159 plant material attracting termite foraging activity and/or stimulating a
160 microbial priming effect (e.g. Lyu *et al.* 2018). To scale up our results and

161 place them in a regional context, we used remote sensing (LiDAR) data to
162 quantify the proportion of canopy openings in the study region and
163 modelled the effect of observed changes in decomposition within gaps on
164 regional carbon flux.

165

166 **Materials and methods**

167 *Study site and gap selection*

168 This study was carried out within an area of lowland, old growth
169 dipterocarp rainforest in the Maliau Basin Conservation Area, Sabah,
170 Malaysia (4° 44' 35" to 55" N and 116° 58' 10" to 30" E; mean annual
171 rainfall 2838 mm \pm 93 mm). On the 20th of July 2017, there was a storm at
172 the study site, which generated winds speeds of 8.4 m/s (Fig. S1). These
173 were among the strongest winds normally experienced in inland forests of
174 the region, which placed extreme sheer stress on trees (Jackson et al.,
175 2020). Consequently, a large number of trees fell within the same 24-hour
176 period in the study location. Ten tree-fall gaps (mean length: 32 m \pm 2.8,
177 mean width: 24.5 m \pm 3; see table S1 for gap characteristics) created
178 during this event were selected for use in this investigation, along with ten
179 adjacent closed canopy sites, located 20 m from the edge of each gap. We
180 took 10 hemispherical photos in each gap and closed canopy sites to
181 quantify canopy openness at each location (see below).

182

183 *Decomposition assay*

184 In October 2017, we established a wood decomposition assay. Using a
185 termite suppression experiment combined with macroinvertebrate

186 accessible and inaccessible mesh bags, Griffiths *et al.* (2019)
187 demonstrated that non-termite macroinvertebrates did not contribute
188 significantly to the decomposition of a standardised wood substrate, *Pinus*
189 *radiata* blocks, at this site. Therefore, to assess the rate of decomposition
190 within these paired gap and closed canopy sites and determine the
191 relative contributions of termites versus microbes to the process, we used
192 the same assay of mass loss from untreated *P. radiata* wood within
193 macroinvertebrate accessible and inaccessible bags. Wood blocks (9 x 9 x
194 5 cm, 161.2 ± 1.3 g; wood density of 0.40 g cm^{-3} [Zanne *et al.*, 2009]; wood C:N
195 ratio of 462 ± 48 [Ganjugunte, Condrón, Clinton, Davis, & Mahieu, 2004])
196 were dried at $60 \text{ }^{\circ}\text{C}$ until they reached a constant weight and placed
197 inside “open” (accessible to macroinvertebrates, principally termites, and
198 microbes), or “closed” (accessible to microbes only) bags, which were all
199 made with 300 micron nylon mesh (Plastok™, Merseyside, UK). The open
200 woodblocks had ten 1 cm holes cut into the top and bottom of the bags to
201 avoid confounding effects of using mesh of different sizes in
202 decomposition assays (Stoklosa *et al.*, 2016). The edges of the closed
203 bags were folded several times and sealed with staples to prevent access
204 by invertebrates. In each gap and closed canopy site, we ran a 50-m
205 transect and randomly placed 5 open and 5 closed wood blocks 5 m apart
206 along the transect ($n = 10$ per site; $n = 200$ woodblocks in total: 10 x
207 forest sites x 2 canopy treatments [closed canopy or gap] x 2 mesh
208 treatments [open or closed] x 5 replicates). Because the gaps were
209 irregular in shape (Appendix table S1), we placed the transects along the
210 longest axis of each gap. In all but one of the gap sites, we were unable to

211 establish a 50 m transect, therefore, we placed an additional line
212 perpendicular to the first, ensuring that each block was always at least 5
213 m apart from its nearest neighbouring block (Fig. 1).

214

215 A hemispherical photograph was taken by placing an iPhone 6 with a
216 fisheye lens attachment directly on top of each wood block. Photographs
217 were analysed using the function *Hemiphot* in R to calculate canopy
218 openness, which was twice as high within the gaps compared with closed
219 canopy sites ($t = 9.67$, $P < 0.001$, mean openness in gap sites = $0.24 \pm$
220 0.03 ; mean openness in closed canopy sites = 0.12 ± 0.02 ; Fig. S2). When
221 placing the woodblocks, the top layer of leaf litter was removed, and the
222 blocks were put directly on the humus layer. Wood blocks were left on the
223 forest floor for 12 months (October 2017 to October 2018), after which
224 they were collected and dried at 60 °C until they reached a constant
225 weight. Once dried, wood material was separated from termite soil. The
226 remaining deadwood and termite material (carton and soil) was then re-
227 weighed separately to calculate the proportion of mass loss from each
228 block and the mass of soil brought into the mesh bags by termites. Given
229 that termites are the only invertebrates known to translocate soil into
230 deadwood (Oberst, Lai, & Evans, 2016), the mass of soil moved into the
231 experimental woodblocks provides additional information on the termite
232 activity compared with non-termite wood-feeding invertebrates.

233

234 *Soil conditions and termite communities*

235 Every month for the 12-month duration of the study, soil moisture
236 percentage and soil temperature were measured within 5 cm of each
237 wood block using a Delta-T Devices HH2 moisture metre (precise to 0.01
238 %) and a digital soil thermometer. Measurements were taken in dry
239 conditions, between 8 AM and 10 AM. To assess termite communities
240 located within the gap and closed canopy sites, we carried out termite
241 transects in September 2018 using the Jones and Eggleton transect
242 method (Jones & Eggleton, 2000). This method uses a 100 m x 2 m belt
243 transect which is divided into twenty 5 m x 1 m sections. Each section is
244 sampled for 30 minutes by two trained collectors searching for termites in
245 twelve 12 cm x 12 cm x 10 cm soil pits and examining all dead wood, leaf
246 litter and trees for the presence of termites. When encountered, termite
247 specimens were collected in 70% ethanol and taken to the laboratory for
248 identification. Because our gap sites were not big enough to place a 100
249 m transect, we carried out the same method but two using smaller
250 transects to equal a 50 m transect combined. Therefore the sampling
251 effort was half that of the Jones & Eggleton (2000) method.

252

253 *Quantifying regional gap area*

254 To assess the size and frequency of gaps within Maliau Basin Conservation
255 Area, we used LiDAR data collected from an airborne survey, which was
256 carried out by the Natural Environment Research Council (NERC) Airborne
257 Research Facility (ARF). In November 2014, a Dornier 228-201 was flown
258 at 1,400-2,400 m a.s.l. with a ground-based Leica base station running
259 simultaneously to allow sub-meter accuracy and georeferencing of the

260 data. Light detection and ranging data were collected using a Leica
261 ALS50-II LiDAR sensor, which emits 120 kHz frequency pulses, has a 12°
262 field of view and a footprint of approximately 40 cm. See Swinfield et al.
263 (2019) for details of LiDAR data processing to generate canopy height and
264 digital terrain models at a 0.5 m resolution. Using these data, we analysed
265 canopy height models to identify gaps, defined as areas with a canopy
266 height of less than 5 m. Gaps larger than 1 ha were filtered out to remove
267 LiDAR artefacts, manmade clearances and the river running through
268 Maliau Basin. We used the package *landscapemetrics* in R and the
269 thresholds described above to detect gaps and to calculate the area of
270 each. We then filtered these results to select only gaps that were between
271 0.025 and 0.16 ha, which is the area range of the gaps forming the basis
272 of this investigation. This allowed us to assess the total area and
273 percentage of the landscape likely to be subject to similar microclimatic
274 conditions to our gap sites at the time of the airborne survey and to
275 quantify the percentage of gaps that are similar in size to those in this
276 study.

277

278 *Dead wood surveys*

279 To estimate the volume of deadwood found on the forest floor in areas
280 affected by tree-fall, compared with undisturbed areas, we carried out
281 deadwood surveys in December 2017. To avoid disturbing our
282 decomposition assays, these surveys were carried out in areas within the
283 forest surrounding experimental plots. We established eight 50 m
284 transects, four of which were within 5 m of a tree that had fallen during

285 the storm in July 2017 and four that were in areas of forest at least 20 m
286 from the nearest tree fall. Along each transect, we recorded the diameter
287 of each piece of deadwood that intersected with the line, and these values
288 were used to calculate the volume of dead wood using the following
289 equation (Van Wagner 1968):

290

$$291 \quad V = \frac{\pi^2}{8L} \sum d^2$$

292

293 Where V is the volume of deadwood ($\text{cm}^3/50 \text{ m}$), d is the diameter of the
294 deadwood item at the intersection and L is the length of the sample line.

295

296 **Carbon Modelling**

297 A bootstrapping scheme with a million simulations was implemented to
298 estimate the carbon flux from dead wood and its uncertainty in Maliau
299 Basin. We estimated carbon fluxes for a completely closed canopy
300 scenario versus scenarios with observed changes in decay rate and
301 deadwood volume in canopy openings as well as canopy gap percentages
302 derived from the remote sensing analysis.

303

304 *Wood density*

305 One species, *Pinus radiata*, was used for estimating wood mass loss in our
306 experiment. Therefore, to account for diversity in wood traits of other
307 species likely to occur at the study site, we used tree survey data from
308 Newbery and Lingenfelder (2004) (collected from a lowland dipterocarp

309 forest site within 100 km of our study site). Our bootstrap analysis used
310 the tree species frequencies from Newbery and Lingenfelder (2004) and
311 selected a wood density for each species from the Global wood density
312 database (Zanne et al., 2009). Where wood density for a species was not
313 available, we randomly selected a wood density value from members of
314 the same genus within the same region category (South-East Asia
315 (tropical)). A histogram of the wood density distribution for this study is
316 shown in Fig. S3. Given that termite and microbial decay rate is negatively
317 associated with wood density in tropical systems (Liu et al., 2015; Mori et
318 al., 2014), this approach reduces the possibility that our model
319 overestimates overall decay rate as a result of the disparity between the
320 density of our decomposition substrate (*P. radiata*: wood density of 0.40 g
321 cm⁻³) and the estimated median density of wood from trees in the study
322 region (0.54 g cm⁻³). We note that the relationship between wood density
323 and decay rate is less clear in temperate forests (Hu et al., 2018; Kahl et
324 al., 2017). In addition to wood density, other traits, such as wood
325 stoichiometry and size of woody substrate (Hu et al., 2018; Kahl et al.,
326 2017; Oberle et al., 2020), are likely to influence decay rates. However,
327 information is lacking on how these other traits affect termite-mediate
328 decay, or wood decomposition more generally in tropical systems.
329 Therefore, we did not incorporate these factors into our models of regional
330 carbon fluxes.

331

332 *Scaling decay rates*

333 Liu et al. (2015) is the only study we know of that quantifies how termite-
334 mediated decay rates depend on wood density. Therefore, we first built a
335 model to represent wood decay rates under termite attack based on Liu et
336 al. (2015). We scaled this model to represent wood decay in gaps using
337 the *P. radiata* wood density and associated decay rate from our study.
338 Then, we scaled the model again to represent these rates under the
339 closed canopy. Wood decay rates in forest gaps were based on Liu et al.
340 (2015) who measured wood traits and decay rates driven by microbes and
341 termites for 66 species. We fitted an exponential model to decay rates as
342 a function of wood density using an L1 scheme that minimizes the sum of
343 the absolute value of the residuals (R package: *L1pack*) (Fig. S4). We used
344 this scheme, rather than a least-squares approach, to avoid over-
345 weighting outliers with high decay rates. To obtain a decay rate for each
346 wood density value, we sampled from a normal distribution with the decay
347 rate model prediction as the mean and the 68%-confidence interval of the
348 model fit as the standard deviation (in log space). To avoid biologically
349 unrealistic decay rates, we truncated the model to the middle 96% of the
350 modelled decay rate estimates (Fig. S4). Because the model derived from
351 Liu et al. (2015) predicted a much higher mean decay rate for *P. radiata*
352 than found in our study (1.3 year⁻¹ compared with 0.49 year⁻¹), we scaled
353 the model to reflect the *P. radiata* decay rates in the canopy gaps open to
354 termite activity that we measured in the field. To predict decay rates
355 under the closed canopy, we also scaled our gap model predictions to
356 match the decay rates of *P. radiata* open to termite decomposition under
357 closed canopy in our study. We accounted for random error in this scaling

358 process by sampling our decay rate dataset with $N(\mu=0.49, \sigma=0.05)$ for
359 the forest gaps and $N(\mu=0.30, \sigma=0.04)$ for the closed canopy to obtain a
360 distribution of scaling factors. These normal distributions were also
361 truncated to the middle 96% quantile.

362

363 *Carbon fluxes*

364 To estimate the deadwood carbon pool at our study site, we used surveys
365 from Pfeifer *et al.* (2015) from nearby Old Growth plot (OG2) of the
366 Stability of Altered Forest Ecosystem (SAFE) project, located within Maliau
367 Basin, <5 km kilometres from our study sites. Pfeifer *et al.* (2015)
368 estimated there to be 10.2 ± 3.5 Mg C per hectare contained in deadwood
369 at the OG2. For the bootstrapping scheme, we sampled 1×10^6 times from
370 a normal distribution of wood pools with the corresponding mean and
371 standard deviation, truncated to the middle 96% quantile. We then
372 estimated carbon fluxes, F , for the closed canopy baseline scenario using
373 the equation

374

$$375 \quad F = k_{canopy} C,$$

376

377 where k_{canopy} is the decay rate per year under the closed canopy and C is
378 the closed canopy carbon pool estimate in megagrams of carbon per
379 hectare. Because the percentage of canopy gaps is small, we assumed
380 that the carbon pool estimates from Pfeifer *et al.* (2015) are
381 representative of the closed canopy. We estimated the carbon flux for our
382 study site, including canopy gaps, using the following equation:

383

$$384 \quad F^{\dot{c}} = p k_{gaps} \alpha C + (1-p) k_{canopy} C,$$

385

386 where $F^{\dot{c}}$ is the flux when gaps are included, p is the proportion of canopy
387 gaps at the study site, k_{gaps} , is the decay rate (yr^{-1}) in the canopy gaps and
388 α is the ratio of the volume of dead wood in the canopy gaps to the
389 volume of dead wood under the closed canopy. Because the sample size
390 was small ($n = 4$, each) for the volume of dead wood in the canopy gaps
391 and under the closed canopy, a normal distribution computed from these
392 data may not be reliable. Therefore, we sampled α directly from the
393 dataset for the bootstrapping scheme. Fluxes are reported as geometric
394 means with geometric standard deviation intervals to best represent the
395 central tendency of the approximately log-normal bootstrapped
396 distributions we obtained.

397

398 **Statistical analysis**

399 A linear mixed effect model (R package: *LmerTest*) was used to determine
400 if wood block bag type (macroinvertebrate accessible vs.
401 macroinvertebrate inaccessible), canopy type (closed canopy vs forest
402 gap) and the interaction between the two factors affected proportion of
403 mass lost from wood blocks. Mass loss was logit transformed, which
404 allowed us to use standard Gaussian linear methods (Warton & Hui, 2011)
405 and forest site was included as a random factor. To carry out multiple
406 comparisons of means and identify any differences in wood block mass
407 loss between bag types and canopy types, we used the *glht* function (R

408 package: *multcomp*) and Tukey contrasts. An Adonis test (package:
409 *vegan*) was used to assess if the community composition of termites
410 differed between the closed canopy and forest gap sites, and zero-inflated
411 generalised linear mixed effects models (R package: *glmmTMB*) were used
412 to test for differences in the encounter rate of each genus separately in
413 the closed canopy and forest sites. Linear mixed effects models were used
414 to test for differences in minimum, mean and maximum soil temperature
415 and moisture values in closed canopy and gap sites; forest site and
416 sampling date were included as random factors. Linear mixed models
417 were used to assess the differences in canopy openness between the
418 closed canopy and forest gaps, with site included as a random factor.

419

420 Finally, to model the relationship between termite-derived soil recovered
421 from the woodblocks and woodblock mass loss, while taking into
422 consideration the high proportion of zeros in the data (50% of open
423 woodblocks contained no termite-derived soil), we analysed the data in a
424 two-stage approach following Min & Agresti (2002). First, we created a
425 binomial variable for the termite soil mass, where woodblocks containing
426 no soil received a 0 and those with more than zero grams of soil received
427 a 1. We then fit the data to a generalised linear mixed effect model
428 (glmer) with site included as a random factor, to test if the proportion of
429 wood mass lost (logit transformed) had a significant effect on the
430 probability of a woodblock containing termite soil. Next, we removed the
431 zero soil values from the dataset and ran a linear mixed effects model
432 (lmer) on only woodblocks from which we recovered soil, to assess if logit

433 transformed wood mass loss was significantly associated with the mass of
434 soil that was recovered from the woodblocks. Again, site was included as
435 a random factor. This approach overcame the problem of modelling zero-
436 inflated data (only invertebrate accessible bags were included in these
437 models because no soil was recovered from closed bags).

438

439 **Results**

440 *Decomposition*

441 Significantly more mass was lost from open woodblocks (accessible to
442 both microbes and macroinvertebrates) in forest gaps (mean mass loss
443 over 12 months: $49\% \pm 5\%$) compared with open woodblocks in closed
444 canopy sites (mean mass loss: $30\% \pm 4\%$; $z = 3.8$, $P < 0.001$). This is an
445 increase in decomposition by a factor of 1.63 in forest where both
446 microbes and macroinvertebrates have access to the woodblocks (Fig. 2).
447 In both the closed canopy and gaps sites, the presence of
448 macroinvertebrates significantly increased the proportion of mass lost, but
449 the magnitude of this increase was greater in forest gaps, as indicated by
450 significant interaction between woodblock bag type and canopy type (LRT
451 $= 4.18$, $P = 0.04$): woodblock mass loss increased by a factor of 2 in open
452 (mean mass loss: $30 \pm 4\%$) compared with closed bags (mean mass loss:
453 $15 \pm 2\%$) in closed canopy sites ($z = 3.08$, $P = 0.01$), but increased by a
454 factor of 2.58 within open (mean mass loss: $49 \pm 5\%$) versus closed bags
455 ($19 \pm 2\%$) in forest gaps ($z = 5.9$, $P < 0.001$). We found a significant
456 positive relationship between woodblock mass loss and the likelihood that
457 a wood block contained termite-derived soil and carton within the open

458 bags ($z = 4.19$, $P < 0.001$; Fig S5), and a significant positive relationship
459 between the proportion of mass lost from a woodblock and the mass of
460 dry soil recovered from bags containing soil ($z = 2.94$, $P = 0.005$; Fig. S5);
461 indicating that termites, rather than other macro-invertebrates, were
462 responsible for this mass loss. There was no significant difference in mass
463 lost from closed woodblocks in the closed canopy compared with closed
464 woodblocks in forest gap sites ($z = 0.86$, $P = 0.83$), suggesting that
465 changes in microbial activity were not responsible for the increase
466 decomposition in the gaps (Fig. 2).

467

468 *Soil microclimate and termite communities*

469 We found small but significant differences in soil temperature and soil
470 moisture within closed canopy and forest gap sites. The soil in gaps
471 tended to be warmer and wetter. Minimum soil temperature was higher by
472 0.5°C and mean soil temperature was 0.3°C higher in gaps compared with
473 closed canopy sites. There was no significant difference in maximum soil
474 temperature. Minimum, mean and maximum soil moisture were higher in
475 canopy gaps compared with non-gap sites by 2, 1.5 and 3.5 percentage
476 points, respectively (Fig. 3; Table 1). We found no difference in the
477 composition of termite communities collected in the closed canopy
478 compared with forest gaps sites nor was there any difference in the
479 number of encounters of individual genera in the two canopy types (Fig.
480 S6).

481

482 *Gap area and carbon modelling*

483 Within the LiDAR surveyed area of 940 ha of lowland tropical rainforest,
484 we detected a total of 20,928 gaps, with the centre of the cumulative
485 distribution of gaps (i.e. the point where half of the gap area is comprised
486 of smaller gaps and the remaining half by larger gaps) at 122 m² (0.01 ha)
487 and covering a cumulative area of 24 ha, or 2.5% of the study site. Of
488 these, 128 gaps were of comparable size to those used in this study
489 (between 0.025 and 0.16 ha). These gaps covered a cumulative area of
490 6.5 ha, which is 0.7 % of the surveyed area and represents 27% of the
491 total gap area in the study region (Fig. 4). In the forest matrix immediately
492 surrounding our experimental plots, we found 187% more deadwood in
493 areas affected by tree fall compared with undisturbed areas (average
494 volume in areas more than 20 m from tree fall: 95.4 ± 36.6 cm³ per 50 m
495 transect; average volume in areas close to tree fall: 272.9 ± 98.7 cm³ per
496 50 m transect; Fig. 5).

497

498 Our initial model applied the changes in decay rate and wood pools to
499 canopy gaps covering 0.7% of the surveyed area, which is the cumulative
500 area that includes gaps of the same size as those forming the basis of this
501 investigation: 128 gaps in total, measuring between 0.025 and 0.16 ha.
502 Under this assumption of gap area, deadwood carbon fluxes increased
503 above baseline by a geometric mean value of 5.7% with a geometric SD
504 interval of -3.1% to 15.2%, corresponding to a flux increase of 0.09 Mg C
505 ha⁻¹ yr⁻¹ (Table 2). If we assumed changes in wood pools and decay rates
506 applied to all gaps detected by LiDAR, i.e. 2.5% of the survey area, then
507 the flux increase was 18.2% (geometric SD interval of -15.4% to 47.7%),

508 or 0.27 Mg C ha⁻¹ yr⁻¹. Increases in both wood pool sizes and termite-
509 driven decay rates in gaps contributed to the higher fluxes relative to the
510 baseline scenario with no gaps (Fig. S10). At the scale of the 940 ha
511 region of our LiDAR analysis, gap-driven fluxes increased from 1380 Mg C
512 ha⁻¹ yr⁻¹ to 1460 Mg C yr⁻¹ for the 0.7% gap scenario and to 1640 Mg C ha⁻¹
513 yr⁻¹ for the 2.5% gap scenario.

514

515 **Discussion**

516 We found that deadwood decomposition in a lowland tropical rainforest
517 increased by approximately two thirds in tree-fall canopy gaps, compared
518 with closed-canopy forest, and that this accelerated decomposition was
519 driven by termites. These results add to a growing body of evidence
520 showing that termites are major drivers of deadwood decomposition in
521 tropical rainforests (Griffiths et al., 2019; Law et al., 2019) and that their
522 importance for the maintenance of ecological processes can increase in
523 response to environmental perturbations (Ashton et al., 2019). The
524 functioning of canopy gaps as hotspots for carbon cycling has important
525 implications for land-surface model development given that tree mortality
526 is increasing in rainforests (Brienen et al., 2015; Hubau et al., 2020;
527 McDowell et al., 2018), which will increase the number of gaps, and
528 cumulative area of forest affected by canopy openings.

529

530

531

532 *Drivers of increased decomposition*

533 We hypothesized that changes in deadwood stocks and microclimate in
534 gaps might alter wood decomposition fluxes. Deadwood stocks were three
535 times higher in canopy gaps than in closed canopy sites. Microbial
536 decomposition did not differ between contrasting canopy conditions while
537 termite-mediated decay increased by almost two thirds in tree-fall gaps.
538 The small but significant differences we detected in the soil microclimate
539 of our gap and closed canopy sites had no effect on microbial decay but
540 may have led to an increase in termite-mediated decay. Combined, these
541 results point to an influx of deadwood foraging material for termites as a
542 likely driver of the increased decomposition in gaps we detected.
543 However, because this hypothesis needs further testing, this work serves
544 as a platform from which the mechanisms behind the patterns we report
545 can be rigorously tested and a starting point for incorporation of these
546 patterns into global carbon models.

547

548 We found no support for our hypothesis that shifts in microclimate and/or
549 disturbance caused by tree mortality are detrimental to the decomposer
550 community. Neither termite nor microbial-mediated wood mass loss
551 declined beneath canopy gaps. Soil conditions in our focal canopy gaps
552 were not as we predicted: although slightly warmer, they were wetter,
553 rather than drier than in the paired closed canopy sites. This result could,
554 in part, explain the lack of disturbance/microclimate effect detected on
555 the decomposer community because we have no *a priori* reason to believe
556 that these small increases in soil moisture would negatively affect
557 microbial or termite activity.

558

559 Our finding of increased termite-mediated decay in canopy gaps supports
560 our alternative hypothesis that an increase in termite food sources
561 (deadwood) in tree fall gaps attracts more termites to these areas, which
562 leads to increased decomposition. We found almost three times more
563 deadwood on the forest floor in areas close to tree fall (Fig. 5), and we
564 propose that this influx of wood is likely to have led to an increase in
565 termite foraging in the gap sites. This finding has important implications
566 for the way in which decomposition models are parameterised in
567 rainforest systems because our results suggest that carbon flux rates from
568 deadwood are not only a function of the proportion of wood necromass in
569 the system (Rice et al., 2004) but may also be mediated by the spatial
570 clustering of the deadwood resource. Given that microbial decay rates did
571 not change in the canopy gaps, we found no evidence to suggest the
572 clustering/influx of dead plant resources had a comparable positive effect
573 on the microbial decomposer community.

574

575 We are confident that termites were responsible for the invertebrate
576 driven increase in decomposition because a previous study, which used
577 macroinvertebrate accessible and inaccessible woodblock bags, in
578 combination with a large-scale suppression of termite communities,
579 demonstrated that non-termite macroinvertebrates do not contribute
580 significantly to wood decay at this site Griffiths et al., (2019). Our present
581 study exactly mimics the experimental design used to manipulate the
582 macroinvertebrate community access to wood blocks in the previous

583 work. Therefore, we conclude that termites were responsible for the
584 elevated mass loss from wood within the macroinvertebrate accessible
585 bags. Moreover, we found a significant positive relationship between the
586 probability that a wood block contained termite-derived soil and
587 proportion wood mass loss, as well as a positive relationship between the
588 mass of soil brought into our open woodblock bags and wood block mass
589 loss (no soil was recovered from closed woodblocks; Fig. S5). This
590 relationship provides further evidence that termites are the main drivers
591 of the observed wood mass loss from the macroinvertebrate accessible
592 bags because termites are the only decomposer organism known to
593 move clay and soil around in this way (Oberst et al., 2016). Because our
594 sampling to assess the composition and biomass of termites within the
595 gap and closed canopy sites was carried out 15-months after the storm
596 that created the focal gaps and influx of deadwood material, it seems
597 likely that we missed the increase in termite activity within the gap sites
598 that we hypothesise led to the elevated decay rate within our gaps.
599 Further work is needed to conclusively disentangle the possible drivers of
600 the increased termite activity and wood decay rates in canopy gaps
601 (microclimate versus increased food supply). Our findings highlight the
602 need to explicitly test the influence of microclimate versus deadwood
603 volume on decay rates in field experiments. This would allow us to gain a
604 deeper understanding of the factors mediating decomposition and carbon
605 balance in rainforest ecosystems.

606

607 *Implications for rainforest carbon flux and sources of uncertainties*

608 We show that termite-mediated deadwood decay responds positively to
609 small-scale disturbances within old-growth rainforest. This suggests that
610 accelerated termite decomposition could be a key driver of observed
611 elevated carbon fluxes caused by increased tree mortality and
612 degradation within standing tropical forests (Baccini et al., 2017; Hubau et
613 al., 2020). As such, these results add to our understanding of the biotic
614 mechanisms underpinning ongoing changes to rainforest carbon budgets.
615 However, the resilience of termite-mediated ecosystem processes to
616 differing disturbance thresholds is largely unknown (but see Tuma *et al.*
617 2019). Recent work has shown that termites maintain leaf litter
618 decomposition, nutrient heterogeneity and soil moisture retention in old
619 growth forest during periods of drought (Ashton et al., 2019), indicating
620 that they can provide ecosystem resilience to climate change.
621 Understanding the extent to which the resilience provided by termites is
622 maintained in degraded habitats is key to the on-going improvement of
623 land-surface models as well the development of land-management
624 practices aimed at increasing the resilience of tropical landscapes under
625 ongoing environmental change

626

627 Given the vast amounts of carbon contained within tropical forests (Lewis,
628 Edwards, & Galbraith, 2015; Pan et al., 2011), even a relatively small
629 change in C flux due to termite-mediated decomposition in canopy gaps
630 may scale up to large differences over tropical biomes. For example, our
631 estimated flux increase of $0.27 \text{ Mg C ha}^{-1} \text{ yr}^{-1}$ represents 2% of total net
632 primary productivity ($13.5 \text{ Mg C ha}^{-1} \text{ yr}^{-1}$) measured in lowland rainforests

633 of Malaysian Borneo (Riutta et al., 2018). This timely finding is of
634 particular relevance given that the Community Land Model version 6
635 (CLM6) is currently under development, which will include additional
636 parameterisation of ecosystem processes that influence the cycling of C
637 through terrestrial ecosystems and build upon progress made in CLM5
638 (Lawrence et al., 2019). However, although our analysis indicated the
639 potential for substantial increases in carbon flux due to changes in termite
640 activity in canopy gaps, the variance around the estimated magnitude of
641 this change in flux remains high due to a number of potential sources of
642 uncertainty in our model.

643

644 Lack of data on how climate mediates the relationship between termite-
645 driven decay and wood density represents an area of uncertainty in our
646 model estimates and contributes to the large confidence intervals
647 associated with our C-flux estimates. Our estimate of termite-mediated
648 decay associated with the varying wood densities is reliant on an
649 empirical model we fitted to a single dataset of decay rates from a distant
650 study site in Yunnan Province, China (Liu et al., 2015). While both are
651 Asian tropical rainforests, the climate differs between the two regions:
652 mean annual rainfall of 1463 mm versus 2838 mm and average monthly
653 temperatures of 21.7°C versus 24.9°C in Yunan (Li et al., 2012) and Maliau
654 (Law et al., 2019), respectively. These climatic differences could be
655 important because while some studies suggest that wood traits are key
656 drivers of deadwood decay (Hu et al., 2018; Zanne et al., 2015), others
657 have found stronger relationships with climate (Chambers, Higuchi,

658 Schimel, Ferreira, & Melack, 2000; Pietsch et al., 2019). Consequently, it is
659 possible that the effect of wood density on rate of termite mediated decay
660 could differ between the two regions.

661

662 Wood density is not the only trait known to influence decay rates. Results
663 from studies focussed on microbial wood decomposition in temperate
664 regions show that a range of other traits can also significantly effect wood
665 decay, either positively (e.g. phosphorous, nitrogen) or negatively (e.g.
666 bark ratio, lignin concentration [Kahl et al., 2017; Oberle et al., 2019]).
667 Furthermore, a recent meta-analysis (Hu et al., 2018), highlighted the
668 importance of wood size (diameter) and nitrogen concentration in
669 controlling wood decay globally. We acknowledge that termite-mediated
670 decay rates could also be influenced by these wood traits and our models
671 may be improved if more data were available on the effect of wood
672 stoichiometry on termite attack rate in our system. However, data on
673 wood chemical traits within our study region are currently unavailable, but
674 Martin, Erickson, Kress, & Thomas (2014) provide an overview of wood
675 nitrogen concentration and correlations between nitrogen and other wood
676 traits for 59 Panamanian tree species. This work reveals a mean wood C:N
677 ratio for these neo-tropical tree species of 278 ± 32 , with values ranging
678 from 84.7 to 1360.8, and a positive relationship between wood density
679 and wood nitrogen concentration. Our wood decomposition substrate
680 (*Pinus radiata*) falls within this range with a C:N of 462 (Ganjegunte et al.,
681 2004).

682

683 We are aware of no study that has interrogated the influence of wood
684 chemical traits on termite mediated decomposition; therefore, we are
685 unable to speculate as to how these factors could influence our flux
686 estimate. However, Ulyshen, Müller, & Seibold (2016) show that termite-
687 mediated wood mass loss increased significantly where bark was present,
688 which is in contrast to the findings presented by Kahl et al., (2017) who
689 show that higher bark ratio negatively affected microbial decay rates. It is
690 important to note that our use of wood blocks of a uniform (small) size
691 and lacking in bark could have resulted in elevated mass loss compared to
692 larger woody substrates with intact bark. However, our wood substrate
693 was chosen to allow for standardization and to facilitate comparison
694 across our experimental sites and treatments. Therefore, we highlight the
695 need for additional work to partition the contributions of microbes versus
696 termites in the decomposition of deadwood with a range of traits and in a
697 range of ecosystems to facilitate the development of more precise models
698 of wood decomposition and carbon cycling.

699

700 Possible inaccuracies in our estimates of deadwood on the forest floor are
701 another potential source of error in our model estimates. We reported that
702 the volume of deadwood was 187% higher in areas affected by treefall
703 compared with those unaffected, using field transects 5-months after the
704 storm that created the canopy gaps. However, it is possible that termite-
705 mediated wood removal in that 5-month period, in response to the influx
706 of foraging material, removed deadwood disproportionately from the tree-
707 fall sites. This would result in an underestimation of the difference in wood

708 volume in contrasting canopy environments, with potentially more
709 deadwood in recently created gaps than we reported. Further, we used
710 data from Pfeifer *et al.* (2015) to describe the deadwood carbon pool
711 under closed canopy conditions. However, Pfeifer *et al.* (2015) reported
712 different deadwood carbon estimates from two sites, both within 3.2 km of
713 our study site (“OG1”: 27.05 Mg C per ha, and “OG2”: 10.24 Mg per ha).
714 We used values from the site closest to our experimental plots (< 1km),
715 OG 2, which was the lowest carbon pool value and thus avoids inflated
716 estimates of the effect of termites on regional C flux. However, the higher
717 deadwood carbon pool reported from Old Growth 1 combined with the
718 possibility that we underestimated the proportional difference in
719 deadwood volume in gaps versus closed canopy sites suggests that our
720 modelling effort is a conservative estimate of the true effect of termite
721 mediated C flux in canopy gaps.

722

723 Finally, difficulties in describing temporally and spatially representative
724 forest canopy gap fractions may have contributed model inaccuracies.
725 Using data from the aerial survey carried out in November 2014, we found
726 the cumulative area of canopy gaps in the study region to be between 0.7
727 and 2.5%. This range is within the lower bounds of canopy gap fractions
728 described by Hunter *et al.* (2015) in the Amazon rainforest (2-5%) and
729 smaller than that reported by Yavitt *et al.* (1995) within a Panamanian
730 forest (4%). Small canopy openings in rainforest ecosystems caused by
731 isolated tree fall events rapidly become colonised by lateral canopy
732 growth, meaning that their detectability using remote sensing quickly

733 decreases with time since gap creation (Asner, Keller, & Silva, 2004). The
734 aerial survey used in this investigation was not, as far as we are aware,
735 carried out soon after an intense storm similar to the storm that created
736 the focal gaps in this study. Therefore, our gap fraction estimate is likely
737 to be smaller than if it been carried out immediately following the storm
738 that formed the basis of this investigation. However, despite these
739 uncertainties, our analysis demonstrates that canopy gaps in rainforest
740 ecosystems function as hotspots of deadwood decay, which has far
741 reaching implications for regional and global budgeting.

742

743 *Conclusion*

744 To our knowledge, this is the first study to show that rainforest treefall
745 canopy gaps represent hotspots for deadwood decay and carbon cycling.
746 We provide insights into the relative importance of invertebrates
747 compared with microbes in driving the decomposition of deadwood,
748 adding to a growing body of literature showing that termites and their
749 mutualistic microbes are equally, if not more important than free-living
750 microorganisms for deadwood decay in rainforests (Griffiths et al., 2019;
751 Law et al., 2019). These results demonstrate that to improve the accuracy
752 of carbon modelling, a variable rate of decomposition should be included
753 in model parameters to account for accelerated termite-mediated decay
754 within tree fall canopy gaps. However, we urgently require information on
755 the effect of a variety of wood traits on termite-mediated decay rates, as
756 well as research efforts to quantify whether these patterns of accelerated
757 decomposition hold true in selectively logged forest or oil palm

758 plantations. Only through addressing these knowledge gaps will we be
759 able to reduce model uncertainties and accurately predict how ongoing
760 changes to tropical landscapes will affect global carbon cycling, climate
761 and the functioning and maintenance of vitally important tropical
762 rainforest ecosystems.

763

764 **Acknowledgements**

765 We are extremely grateful to our field assistants R. Binti Manber, Lawlina
766 Mansul and Donny Banasib for their tireless hard work in the field, which
767 made this study possible. We thank G. Reynolds, U. Jami and A. Karolus
768 for coordinating fieldwork. This work was supported by the South East
769 Asian Rainforest Research Partnership (SEARRP), with permission from
770 Maliau Basin Management Committee and the Sabah Biodiversity Council.
771 We thank the funding bodies that financially supported this work: The
772 Leverhulme Trust, research grant: RPG-2017-271 awarded to KP; National
773 Science Foundation, Research Traineeship 1633631 to NHS, and National
774 Science Foundation, grant DEB-1655340 to SDA.

775

776 **Data Sharing and Accessibility**

777 The data that support the findings of this study are openly available in
778 Dryad data repository at [http://doi.org/\[doi\]](http://doi.org/[doi]), reference number [reference
779 number].

780

781 **References**

782 Allen, C. D., Breshears, D. D., & McDowell, N. G. (2015). On

783 underestimation of global vulnerability to tree mortality and forest die-
784 off from hotter drought in the Anthropocene. *Ecosphere*, 6(8), 1–55.
785 <https://doi.org/10.1890/ES15-00203.1>

786 Ashton, L. A., Griffiths, H. M., Parr, C. L., Evans, T. A., Didham, R. K.,
787 Hasan, F., ... Eggleton, P. (2019). Termites mitigate the effects of
788 drought in tropical rainforest. *Science*, 177(January), 174–177.

789 Asner, G. P., Keller, M., & Silva, J. N. M. (2004). Spatial and temporal
790 dynamics of forest canopy gaps following selective logging in the
791 eastern Amazon. *Global Change Biology*, 10(5), 765–783.
792 <https://doi.org/10.1111/j.1529-8817.2003.00756.x>

793 Baccini, A., Walker, W., Carvalho, L., Farina, M., Sulla-Menashe, D., &
794 Houghton, R. A. (2017). Tropical forests are a net carbon source based
795 on aboveground measurements of gain and loss. *Science*,
796 358(October), 230–234.

797 Blonder, B., Both, S., Coomes, D. A., Elias, D., Jucker, T., Kvasnica, J., ...
798 Svátek, M. (2018). Extreme and Highly Heterogeneous Microclimates
799 in Selectively Logged Tropical Forests. *Frontiers in Forests and Global*
800 *Change*, 1(October), 1–14. <https://doi.org/10.3389/ffgc.2018.00005>

801 Bodman, R. W., Rayner, P. J., & Karoly, D. J. (2013). Uncertainty in
802 temperature projections reduced using carbon cycle and climate
803 observations. *Nature Climate Change*, 3(8), 725–729.
804 <https://doi.org/10.1038/nclimate1903>

805 Brienen, R. J. W., Phillips, O. L., Feldpausch, T. R., Gloor, E., Baker, T. R.,
806 Lloyd, J., ... Zagt, R. J. (2015). Long-term decline of the Amazon carbon
807 sink. *Nature*, 519(7543), 344–348.

808 <https://doi.org/10.1038/nature14283>

809 Cai, W., Borlace, S., Lengaigne, M., Van Rensch, P., Collins, M., Vecchi, G.,
810 ... Jin, F. F. (2014). Increasing frequency of extreme El Niño events due
811 to greenhouse warming. *Nature Climate Change*, 4(2), 111–116.
812 <https://doi.org/10.1038/nclimate2100>

813 Carlson, B. S., Koerner, S. E., Medjibe, V. P., White, L. J. T., & Poulsen, J. R.
814 (2017). Deadwood stocks increase with selective logging and large
815 tree frequency in Gabon. *Global Change Biology*, 23(4), 1648–1660.
816 <https://doi.org/10.1111/gcb.13453>

817 Chambers, J. Q., Higuchi, N., Schimel, J. P., Ferreira, L. V, & Melack, J. M.
818 (2000). Decomposition and carbon cycling of dead trees in tropical
819 forests of the central Amazon. *Oecologia*, 122(3), 380–388.
820 <https://doi.org/10.1007/s004420050044>

821 Cornwell, W. K., Cornelissen, J. H. C., Allison, S. D., Bauhus, J., Eggleton, P.,
822 Preston, C. M., ... Zanne, A. E. (2009). Plant traits and wood fates
823 across the globe: Rotted, burned, or consumed? *Global Change*
824 *Biology*, 15(10), 2431–2449. [https://doi.org/10.1111/j.1365-](https://doi.org/10.1111/j.1365-2486.2009.01916.x)
825 [2486.2009.01916.x](https://doi.org/10.1111/j.1365-2486.2009.01916.x)

826 da Costa, R. R., Hu, H., Li, H., & Poulsen, M. (2019). Symbiotic plant
827 biomass decomposition in Fungus-Growing termites. *Insects*, 10(4), 1–
828 15. <https://doi.org/10.3390/insects10040087>

829 Dibog, L., Eggleton, P., Norgrove, L., Bignell, D. E., & Hauser, S. (1999).
830 Impacts of canopy cover on soil termite assemblages in an
831 agrisilvicultural system in southern Cameroon. *Bulletin of*
832 *Entomological Research*, 89(02), 125–132.

833 <https://doi.org/10.1017/S0007485399000206>

834 Eggleton, P., Bignell, D. E., Sands, W. A., Waite, B., Wood, T. G., & Lawton,
835 J. H. (1995). The species richness of termites (isoptera) under differing
836 levels of forest disturbance in the mbalmayo forest reserve, southern
837 cameroon. *Journal of Tropical Ecology*, 11(1), 85–98.
838 <https://doi.org/10.1017/S0266467400008439>

839 Ewers, R. M., Boyle, M. J. W., Gleave, R. A., Plowman, N. S., Benedick, S.,
840 Bernard, H., ... Turner, E. C. (2015). Logging cuts the functional
841 importance of invertebrates in tropical rainforest. *Nature*
842 *Communications*, 6, 6836. <https://doi.org/10.1038/ncomms7836>

843 Ganjegunte, G. K., Condrón, L. M., Clinton, P. W., Davis, M. R., & Mahieu,
844 N. (2004). Decomposition and nutrient release from radiata pine
845 (*Pinus radiata*) coarse woody debris. *Forest Ecology and Management*,
846 187(2–3), 197–211. [https://doi.org/10.1016/S0378-1127\(03\)00332-3](https://doi.org/10.1016/S0378-1127(03)00332-3)

847 Griffiths, H. M., Ashton, L. A., Evans, T. A., Parr, C. L., & Eggleton, P.
848 (2019). Termites can decompose more than half of deadwood in
849 tropical rainforest. *Current Biology*, 29, 118–119.
850 <https://doi.org/10.1016/j.cub.2019.01.012>

851 Hardwick, S. R., Toumi, R., Pfeifer, M., Turner, E. C., Nilus, R., & Ewers, R.
852 M. (2015). The relationship between leaf area index and microclimate
853 in tropical forest and oil palm plantation: Forest disturbance drives
854 changes in microclimate. *Agricultural and Forest Meteorology*, 201,
855 187–195. <https://doi.org/10.1016/j.agrformet.2014.11.010>

856 Harmon, M. E., Bond-Lamberty, B., Tang, J., & Vargas, R. (2011).
857 Heterotrophic respiration in disturbed forests: A review with examples

858 from North America. *Journal of Geophysical Research: Biogeosciences*,
859 116(2), 1-17. <https://doi.org/10.1029/2010JG001495>

860 Harmon, M. E., Fasth, B. G., Yatskov, M., Kastendick, D., Rock, J., &
861 Woodall, C. W. (2020). Release of coarse woody detritus - related
862 carbon : a synthesis across forest biomes. *Carbon Balance and*
863 *Management*, 1-21. <https://doi.org/10.1186/s13021-019-0136-6>

864 Hu, Z., Michaletz, S. T., Johnson, D. J., McDowell, N. G., Huang, Z., Zhou,
865 X., & Xu, C. (2018). Traits drive global wood decomposition rates more
866 than climate. *Global Change Biology*, 24(11), 5259-5269.
867 <https://doi.org/10.1111/gcb.14357>

868 Hubau, W., Lewis, S. L., Phillips, O. L., Affum-Baffoe, K., Beeckman, H.,
869 Cuní-Sanchez, A., ... Zemagho, L. (2020). Asynchronous carbon sink
870 saturation in African and Amazonian tropical forests. *Nature*,
871 579(7797), 80-87. <https://doi.org/10.1038/s41586-020-2035-0>

872 Hunter, M. O., Keller, M., Morton, D., Cook, B., Lefsky, M., Ducey, M., ...
873 Zang, R. (2015). Structural dynamics of tropical moist forest gaps.
874 *PLoS ONE*, 10(7), 1-19. <https://doi.org/10.1371/journal.pone.0132144>

875 Jackson, T. ., Shenkin, A. ., Majalap, N., Jami, J. ., Sailim, A. B., Reynolds,
876 G., ... Disney, M. (2020). The mechanical stability of the world's tallest
877 broadleaf trees. *The Mechanical Stability of the World's Tallest*
878 *Broadleaf Trees*, 00, 1-11. <https://doi.org/10.1101/664292>

879 Janisch, J. E., Harmon, M. E., Chen, H., Fasth, B., & Sexton, J. (2005).
880 Decomposition of coarse woody debris originating by clearcutting of
881 an old-growth conifer forest. *Écoscience*, 12(2), 151-160.
882 <https://doi.org/10.2980/i1195-6860-12-2-151.1>

883 Jones, D. T., & Eggleton, P. (2000). Sampling termite assemblages in
884 tropical forests: Testing a rapid biodiversity assessment protocol.
885 *Journal of Applied Ecology*, 37(1), 191–203.
886 <https://doi.org/10.1046/j.1365-2664.2000.00464.x>

887 Kahl, T., Arnstadt, T., Baber, K., Bässler, C., Bauhus, J., Borken, W., ...
888 Gossner, M. M. (2017). Wood decay rates of 13 temperate tree species
889 in relation to wood properties, enzyme activities and organismic
890 diversities. *Forest Ecology and Management*, 391, 86–95.
891 <https://doi.org/10.1016/j.foreco.2017.02.012>

892 Law, S., Eggleton, P., Griffiths, H., Ashton, L., & Parr, C. (2019). Suspended
893 Dead Wood Decomposes Slowly in the Tropics , with Microbial Decay
894 Greater than Termite Decay. *Ecosystems*, (June).
895 <https://doi.org/10.1007/s10021-018-0331-4>

896 Lawrence, D. M., Fisher, R. A., Koven, C. D., Oleson, K. W., Swenson, S. C.,
897 Bonan, G., ... Zeng, X. (2019). The Community Land Model Version 5:
898 Description of New Features, Benchmarking, and Impact of Forcing
899 Uncertainty. *Journal of Advances in Modeling Earth Systems*, 11(12),
900 4245–4287. <https://doi.org/10.1029/2018MS001583>

901 Lewis, S. L., Edwards, D. P., & Galbraith, D. (2015). Increasing human
902 dominance of tropical forests. *Science*, 349, 827–832.

903 Li, R., Luo, G., Meyers, P. A., Gu, Y., Wang, H., & Xie, S. (2012). Leaf wax n-
904 alkane chemotaxonomy of bamboo from a tropical rain forest in
905 Southwest China. *Plant Systematics and Evolution*, 298(4), 731–738.
906 <https://doi.org/10.1007/s00606-011-0584-2>

907 Liu, G., Cornwell, W. K., Cao, K., Hu, Y., Van, R. S. P., Yang, S., ...

908 Cornelissen, J. H. C. (2015). Termites amplify the effects of wood traits
909 on decomposition rates among multiple bamboo and dicot woody
910 species. *Journal of Ecology*, *103*, 1214–1223.
911 <https://doi.org/10.1111/1365-2745.12427>

912 Luke, S. H., Fayle, T. M., Eggleton, P., Turner, E. C., & Davies, R. G. (2014).
913 Functional structure of ant and termite assemblages in old growth
914 forest, logged forest and oil palm plantation in Malaysian Borneo.
915 *Biodiversity and Conservation*, *23*(11), 2817–2832.
916 <https://doi.org/10.1007/s10531-014-0750-2>

917 Lyu, M., Xie, J., Vadeboncoeur, M. A., Wang, M., Qiu, X., Ren, Y., ...
918 Kuzyakov, Y. (2018). Simulated leaf litter addition causes opposite
919 priming effects on natural forest and plantation soils. *Biology and*
920 *Fertility of Soils*, *54*(8), 925–934. [https://doi.org/10.1007/s00374-018-](https://doi.org/10.1007/s00374-018-1314-5)
921 [1314-5](https://doi.org/10.1007/s00374-018-1314-5)

922 Martin, A. R., Erickson, D. L., Kress, W. J., & Thomas, S. C. (2014). Wood
923 nitrogen concentrations in tropical trees: phylogenetic patterns and
924 ecological correlates. *New Phytologist*, *205*, 484–495.

925 McDowell, N., Allen, C. D., Anderson-Teixeira, K., Brando, P., Brienen, R.,
926 Chambers, J., ... Xu, X. (2018). Drivers and mechanisms of tree
927 mortality in moist tropical forests. *New Phytologist*, *219*(3), 851–869.
928 <https://doi.org/10.1111/nph.15027>

929 Min, Y., & Agresti, A. (2002). Modeling Nonnegative Data with Clumping at
930 Zero : A Survey Models for Semicontinuous Data. *Jirss*, *1*(May), 7–33.

931 Mori, S., Itoh, A., Nanami, S., Tan, S., Chong, L., & Yamakura, T. (2014).
932 Effect of wood density and water permeability on wood decomposition

933 rates of 32 bornean rainforest trees. *Journal of Plant Ecology*, 7(4),
934 356–363. <https://doi.org/10.1093/jpe/rtt041>

935 Newbery, D. M., & Lingenfelder, M. (2004). Resistance of a lowland rain
936 forest to increasing drought intensity in Sabah, Borneo. *Journal of*
937 *Tropical Ecology*, 20(6), 613–624.
938 <https://doi.org/10.1017/S0266467404001750>

939 Oberle, B., Lee, M. R., Myers, J. A., Osazuwa-Peters, O. L., Spasojevic, M. J.,
940 Walton, M. L., ... Zanne, A. E. (2020). Accurate forest projections
941 require long-term wood decay experiments because plant trait effects
942 change through time. *Global Change Biology*, 26(2), 864–875. [https://](https://doi.org/10.1111/gcb.14873)
943 doi.org/10.1111/gcb.14873

944 Oberle, B., Lee, M. R., Myers, J. A., Osazuwa-Peters, O. L., Spasojevic, M. J.,
945 Walton, M. L., ... Zanne, A. E. (2019). Accurate forest projections
946 require long-term wood decay experiments because plant trait effects
947 change though time. *Global Change Biology*, (October), 1–12.
948 <https://doi.org/10.1111/gcb.14873>

949 Oberst, S., Lai, J. C. S., & Evans, T. A. (2016). Termites utilise clay to build
950 structural supports and so increase foraging resources. *Scientific*
951 *Reports*, 6(September 2015), 1–11. <https://doi.org/10.1038/srep20990>

952 Pan, Y., Birdsey, R. a, Fang, J., Houghton, R., Kauppi, P. E., Kurz, W. a, ...
953 Hayes, D. (2011). A large and persistent carbon sink in the world's
954 forests. *Science*, 333(6045), 988–993.
955 <https://doi.org/10.1126/science.1201609>

956 Pfeifer, M., Lefebvre, V., Turner, E., Cusack, J., Khoo, M. S., Chey, V. K., ...
957 Ewers, R. M. (2015). Deadwood biomass: An underestimated carbon

958 stock in degraded tropical forests? *Environmental Research Letters*,
959 10(4). <https://doi.org/10.1088/1748-9326/10/4/044019>

960 Pietsch, K. A., Eichenberg, D., Nadrowski, K., Bauhus, J., Buscot, F.,
961 Purahong, W., ... Wirth, C. (2019). Wood decomposition is more
962 strongly controlled by temperature than by tree species and
963 decomposer diversity in highly species rich subtropical forests. *Oikos*,
964 128(5), 701–715. <https://doi.org/10.1111/oik.04879>

965 Rice, A. H., Pyle, E. H., Saleska, S. R., Hutyra, L., Palace, M., Keller, M., ...
966 Wofsy, S. C. (2004). Carbon balance and vegetation dynamics in an
967 old-growth Amazonian forest. *Ecological Applications*, 14(4), 55–71.
968 <https://doi.org/10.1890/02-6006>

969 Riutta, T., Malhi, Y., Kho, L. K., Marthews, T. R., Huaraca Huasco, W., Khoo,
970 M. S., ... Ewers, R. M. (2018). Logging disturbance shifts net primary
971 productivity and its allocation in Bornean tropical forests. *Global*
972 *Change Biology*, 24(7), 2913–2928. <https://doi.org/10.1111/gcb.14068>

973 Shorohova, E., & Kapitsa, E. (2014). Influence of the substrate and
974 ecosystem attributes on the decomposition rates of coarse woody
975 debris in European boreal forests. *Forest Ecology and Management*,
976 315, 173–184. <https://doi.org/10.1016/j.foreco.2013.12.025>

977 Stoklosa, A. M., Ulyshen, M. D., Fan, Z., Varner, M., Seibold, S., & Müller, J.
978 (2016). Effects of mesh bag enclosure and termites on fine woody
979 debris decomposition in a subtropical forest. *Basic and Applied*
980 *Ecology*, 17(5), 463–470. <https://doi.org/10.1016/j.baae.2016.03.001>

981 Swift, M. J. (1977). The ecology of wood decomposition. *Science Progress*,
982 64(254), 175–199. Retrieved from

983 <http://www.bcin.ca/Interface/openbcin.cgi?>
984 [submit=submit&Chinkey=35034](http://www.bcin.ca/Interface/openbcin.cgi?submit=submit&Chinkey=35034)

985 Swinfield, T., Both, S., Riutta, T., Bongalov, B., Elias, D., Majalap-Lee, N., ...
986 Coomes, D. (2019). Imaging spectroscopy reveals the effects of
987 topography and logging on the leaf chemistry of tropical forest canopy
988 trees. *Global Change Biology*, (October), 1-14. [https://doi.org/10.1111/](https://doi.org/10.1111/gcb.14903)
989 [gcb.14903](https://doi.org/10.1111/gcb.14903)

990 Tuma, J., Fleiss, S., Eggleton, P., Frouz, J., Klimes, P., Lewis, O. T., ... Fayle,
991 T. M. (2019). Logging of rainforest and conversion to oil palm reduces
992 bioturbator diversity but not levels of bioturbation. *Applied Soil*
993 *Ecology*, 144(August), 123-133.
994 <https://doi.org/10.1016/j.apsoil.2019.07.002>

995 Ulyshen, M. D., Müller, J., & Seibold, S. (2016). Bark coverage and insects
996 influence wood decomposition : Direct and indirect effects. *Applied*
997 *Soil Ecology*, 105, 25-30. <https://doi.org/10.1016/j.apsoil.2016.03.017>

998 Van Wagner C.E. (1968). The Line Intersect Method in Forest Fuel
999 Sampling. *Forest Science*, 14(1), 20-26.

1000 Warton, D. I., & Hui, F. K. C. (2011). The arcsine is asinine: the analysis of
1001 proportions in ecology. *Ecology*, 92(1), 3-10.

1002 Yavitt, J. B., Battles, J. J., Lang, G. E., & Knight, D. H. (1995). The Canopy
1003 Gap Regime in a Secondary Neotropical Forest in Panama. *Journal of*
1004 *Tropical Ecology*, 11(3), 391-402.

1005 Yavitt, J. B., Wright, S. J., & Wieder, R. K. (2004). Seasonal drought and
1006 dry-season irrigation influence leaf-litter nutrients and soil enzymes in
1007 a moist, lowland forest in Panama. *Austral Ecology*, 29(2), 177-188.

1008 <https://doi.org/10.1111/j.1442-9993.2004.01334.x>

1009 Zanne, A. E., Lopez-Gonzalez, G., Coomes, D. A., Llic, J., Jansen, S., Lewis,
 1010 S. L., ... Chave, J. (2009). Global wood density database. *Dryad*.

1011 Zanne, A. E., Oberle, B., Dunham, K. M., Milo, A. M., Walton, M. L., &
 1012 Young, D. F. (2015). A deteriorating state of affairs: How endogenous
 1013 and exogenous factors determine plant decay rates. *Journal of*
 1014 *Ecology*, 103(6), 1421-1431. <https://doi.org/10.1111/1365-2745.12474>

1015
 1016
 1017
 1018
 1019
 1020

1021 **Tables**

1022 **Table 1.** Mean soil temperature and moisture in closed canopy and forest
 1023 gap sites and outputs from linear mixed effects models to assess the
 1024 effect of gaps on soil conditions (asterisks indicate significant differences
 1025 between closed canopy and gap sites).

Microclimate metric	Mean value		Forest		t- value	P
	Closed canopy		gap			
Min. soil temp. (°C)	7 24.0	± 0.22	5 24.4	± 0.17	2.56	0.01* 0.001
Mean soil temp. (°C)	9 25.1	± 0.07	0 25.3	± 0.07	3.22	**
Max soil temp. (°C)	3	± 0.10	8	± 0.09	1.38	0.17
Min. soil moisture	12.9	± 0.39	14.0	± 0.24	2.28	0.02*

(%)			0		6			
Mean	soil	moisture	19.5		20.9			
(%)			0	± 0.44	5	± 0.48	2.65	0.01*
Max	soil	moisture	26.7		30.2			0.001
(%)			7	± 0.58	6	± 0.76	3.37	**

1026
1027
1028
1029
1030
1031
1032
1033
1034
1035
1036
1037

1038 **Table 2.** Estimates of geometric mean carbon fluxes and standard
1039 deviation intervals (square brackets) based on 1×10^6 simulations for the
1040 following scenarios: a closed canopy baseline; a scenario with 0.7% forest
1041 gap, which, based on the LiDAR data, is the cumulative percentage of
1042 forest area that is a gap of the same size as our focal experimental gaps
1043 (between 0.025 and 0.16 ha); and a scenario with 2.5% forest gap, which
1044 is the total (maximum) proportion of forest that was classified as a gap in
1045 the LiDAR survey.

	Baseline	0.7% gaps	Forest 2.5% gaps	Forest
--	----------	--------------	------------------------	--------

Carbon flux (Mg C ha ⁻¹ yr ⁻¹)	1.47 [0.57, 3.83]	1.56 [0.61, 3.96]	1.74 [0.70, 4.32]
Ratio to baseline	1.000	1.057 [0.969, 1.152]	1.182 [0.846, 1.477]
Carbon flux for LiDAR region (Mg C yr ⁻¹)	1380 [530, 3600]	1460 [570, 3720]	1640 [660, 4060]

1046

1047

1048 **Figure legends**

1049

1050 **Figure 1.** Schematic diagram of the study experimental design. In

1051 October 2017, we selected 10 canopy gaps (mean width 24.5 m, mean

1052 length 32 m), created by tree-fall during a storm even in July 217, and 10

1053 paired closed canopy sites (located 20 m from the edge of each gap).

1054 Within each gap and closed canopy site, we randomly placed 5 x

1055 invertebrate accessible woodblocks (represented by the grey boxes) and 5

1056 x invertebrate inaccessible woodblock (yellow boxes). Each woodblock

1057 was separated by at least 5 m and was left on the forest floor for 12-

1058 months.

1059

1060 **Figure 2.** Median plus interquartile range for mass loss from

1061 macroinvertebrate accessible (grey boxes) and macroinvertebrate

1062 inaccessible (yellow boxes) wood blocks within closed canopy and tree-fall

1063 gaps. Points are the raw data are displayed over the boxes.

1064

1065 **Figure 3.** Frequency distributions of minimum, mean and maximum soil
1066 temperature (panels a, c, e) and soil moisture (panels b, d, f) within closed
1067 canopy (grey ribbons) and forest gaps (yellow ribbons). Vertical dashed
1068 lines indicate significant differences between mean microclimate
1069 attributes in the different canopy types (closed canopy: grey lines, forest
1070 gaps: yellow lines).

1071

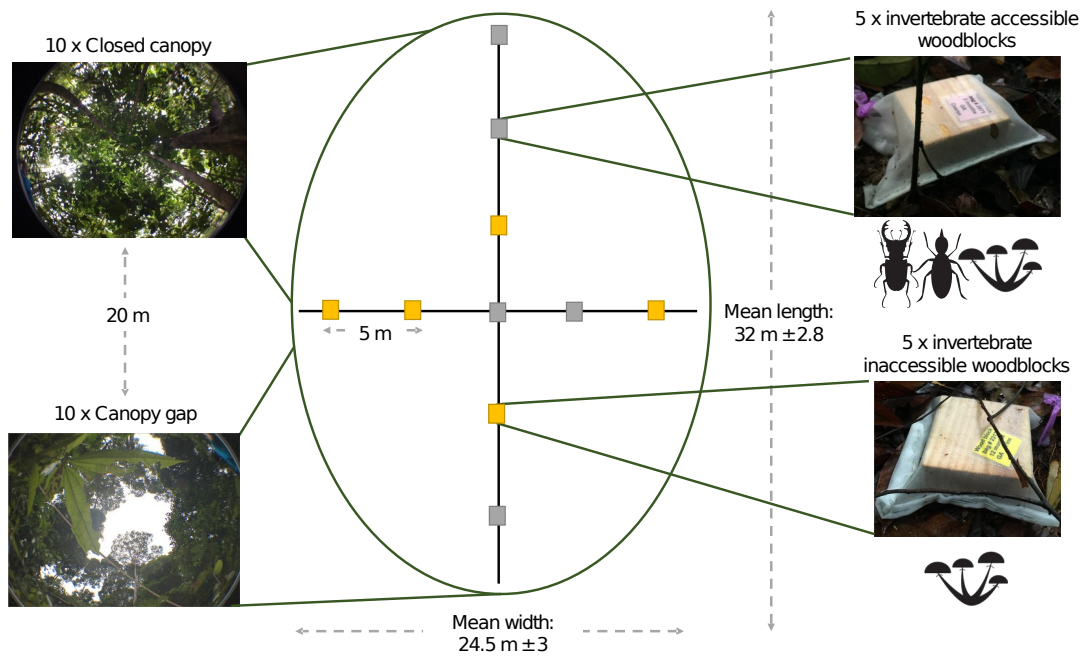
1072 **Figure 4.** Cumulative distribution of canopy gap area. Gaps of the same
1073 area as those forming the basis of this investigation (128 gaps, between
1074 0.025 and 0.16 ha) fall within the yellow rectangle. The total area
1075 represented by the yellow rectangle is 6.5 ha, which is 0.7 % of the
1076 surveyed area and represents 27% of the total gap area in the study
1077 region. The vertical dashed line at 122 m² (0.01 ha) represents the centre
1078 of the cumulative distribution function, where half of the gap area is
1079 comprised of smaller gaps and the remaining half by larger gaps.

1080

1081 **Figure 5.** Median (horizontal lines) plus 95% confidence intervals
1082 (whiskers) of the volume of deadwood on the forest floor beneath closed
1083 canopy (grey box) and sites within 5 m of a canopy gap.

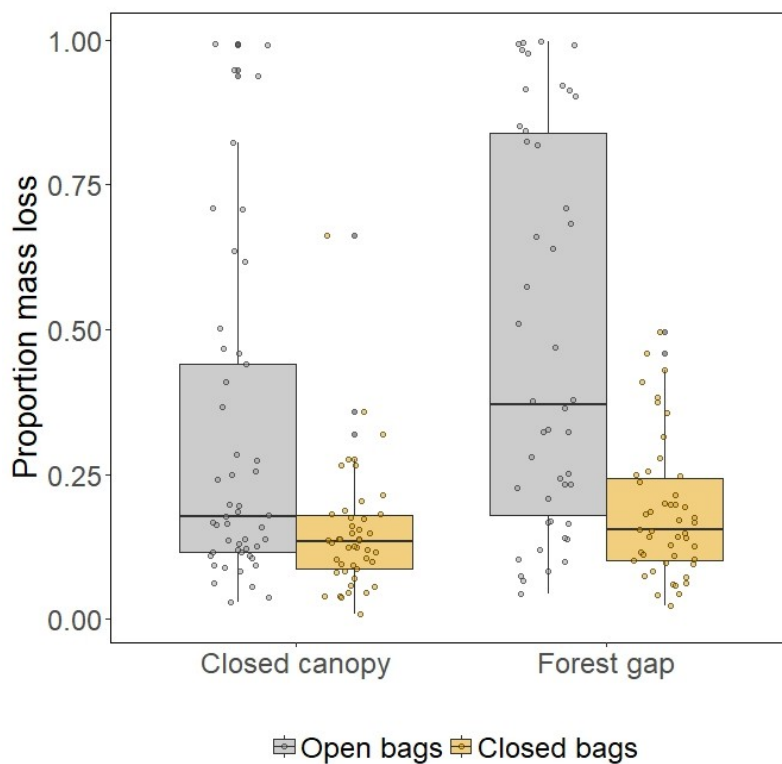
1084

1085



1086

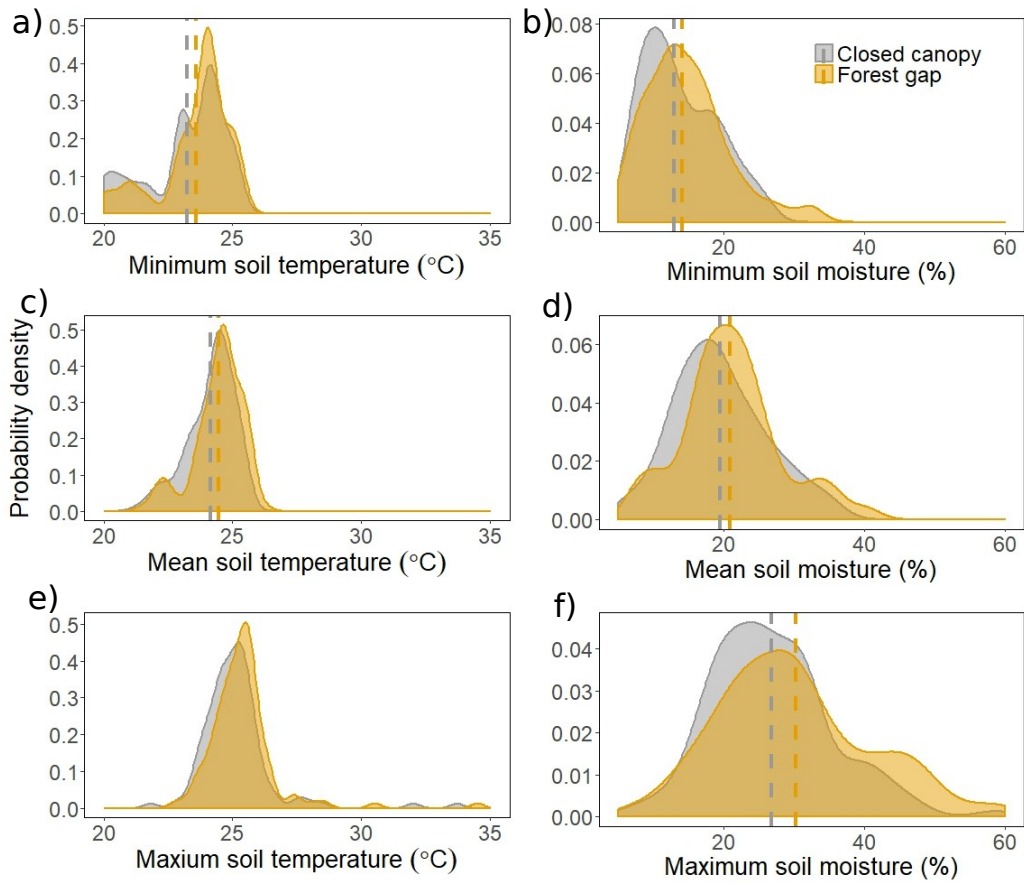
1087 **Figure 1.**



1088

1089 **Figure 2.**

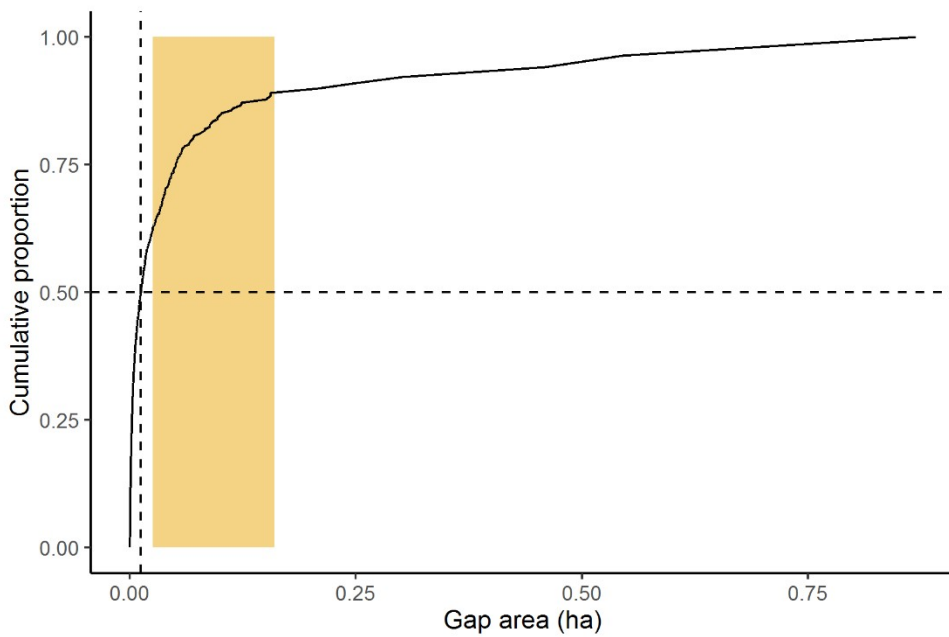
1090



1091

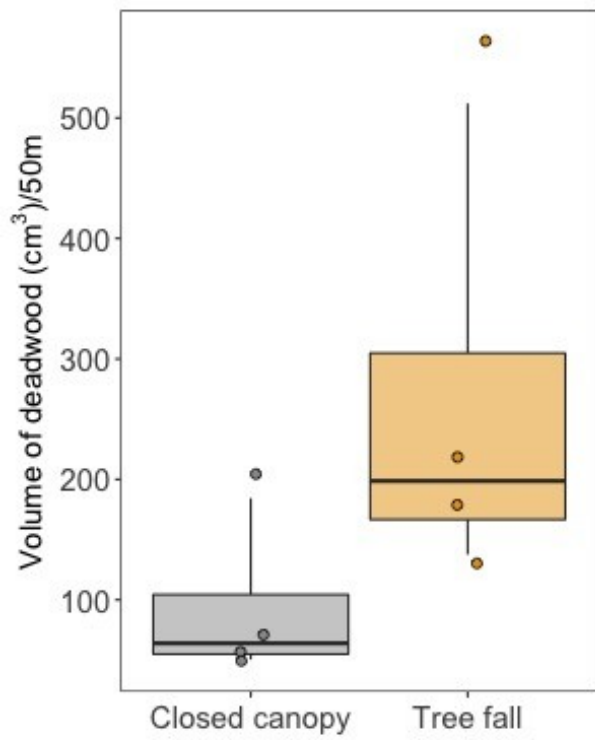
1092 **Figure. 3**

1093



1094

1095 **Figure 4.**



1096

1097 **Figure 5.**